International Journal of Signal Processing, Image Processing and Pattern Recognition
Vol. 8, No. 2 (2015), pp. 105-114
http://dx.doi.org/10.14257/ijsip.2015.8.2.11

Phase Sensitivity to Acoustic Pressure of Microstrustured Optical Fibers: A comparison Study

Adel Abdallah, Zhang Chaozhu and Zhong Zhi

College of information and communication engineering, Harbin Engineering University, Heilongjiang province, Harbin City, 150001, P.R. China
adelmtc39@gmail.com, zhangchaozhu@hrbeu.edu.cn, zhongzhi@hrbeu.edu.cn

Abstract

Recently, photonic crystal fibers (PCFs) have attracted many researchers because of their unique properties, and design flexibility that can't be realized by conventional fibers. One of the fruitful areas of research is the optical fiber hydrophone. In this paper, the finite element solver (FES), COMSOL multiphysics, is used to study and compare the response to acoustic pressure of a hollow-core photonic band gap fiber (HC-PBF), a solid-core photonic crystal fiber (SC-PCF), and a conventional single-mode fiber (SMF) for different acoustic pressures in the frequency range from 10 kHz to 50 kHz. The key structural factors affect the sensitivity to acoustic pressure (S) of the microstructured fibers are studied and a mathematical formula describes the relation of S and the dominant structural factor is proposed. Simulation results of the investigated optical fibers show that the normalized responsivity (NR) of the HC-1550, LMA-5, and SMF are -344 dB, -367.5 dB, and -366 dB, respectively. The proposed simulation results are in good agreement with published theoretical and experimentally measured results. The proposed results indicate the significance of the HC-PBFs in the future hydrophone systems and are useful for the design of microstrustured optical fibers for sensing applications.

Keywords: *Hollow-core photonic bandgap fiber, Microstructured silica fiber, Optical fiber acoustic sensors, Normalized acoustic responsivity, Optical fiber hydrophone*

1. Introduction

For many years, researchers have shown the advantages of the SMF hydrophones as a potential alternative to the existing sound navigation and ranging (SONAR) technology [1, 2]. The SMF hydrophone has low acoustic sensitivity because it is made of glass material that has high Young's modulus makes them incompressible. In addition, the refractive index change due to fiber strain has opposite sign with respect to length change and hence reduces NR [3]. Searching for better performance, researchers tested photonic crystal fibers (PCFs) that can be divided into two categories; SC-PCFs in which light is guided by modified total internal reflection, and HC-PBFs in which light is guided by the photonic bandgap effect. Previous work showed that SC-PCF has about the same performance as that of SMF as acoustic sensor [4]. However, SC-PCFs sensors showed excellent performance in many applications. This is because they offer attractive advantages over SMFs such as the design flexibility, endlessly single-mode operation, the possibility to fabricate sensors based on refractive index change by filling its air holes with materials or liquids, and they are almost insensitive to bending allows the fabication of hydrophones with larger number of arrays, smaller size and lower cost [5-7]. It was reported that large mode area (LMA-5) PCF, beside other advantages, is almost bend insenstive in the studied spectral range from 400 nm to 1000 nm up to bend diameter of 1 cm, that can be used to realize smaller hydrophone size [5, 8]. The aforementioned

ISSN: 2005-4254 IJSIP

advantages motivated us to study the feasibility of using LMA-5 in the optical hydrophones.

HC-PBF were tested experimentally as interferometric acoustic sensors and it was found out that it has many advantages over SMF that contribute to better sensitivity to measurands and suitability for many applications [3, 5, 9, 10]. Some of these advantages are; (1) design and manufacturing flexibility of HC-PBFs can reduce the effective Young's modulus of the fiber and enhances the NR of the HC-PBF [3, 11], (2) the undesirable negative index effect introduced in SMF is expected to be greatly reduced in a HC-PBF in which most of the mode energy is confined in air, so the NR of the HC-PBF is expected to have higher sensitivity, (3) holes of the HC-PBF can be filled with a material with opposite thermal expansion to make the material completely temperature insensitive [9], (4) In the HC-PBF sensing coil, because the light travels through air, it has much smaller Kerr, Faraday, and thermal constants than silica cores, this reduces the dependencies on power, magnetic field, and temperature fluctuations [9], (5) HC-PBFs are almost entirely bend-insensitive and can be bent down to very small diameters (<1cm) with minimal loss, this makes it suitable for small-size hydrophone applications [5, 12], and (6) HC-PBFs have very low back-reflection at the fiber end faces because of the close match of the mode index with the ambient air and this helps to reduce the back-reflected light level which is beneficial for many applications [10]. However, using PCFs as acoustic sensors needs further investigation to be feasible as an alternative to its counterpart of SMF interferometers. In this paper, the finite element solver COMSOL multiphysics, is used to study the response to acoustic pressure (p) of HC-1550 as HC-PBF, large-mode area (LMA-5) as SC-PCF, and the conventional SMF. The effect of the main structural factors of the PCFs on its NR were studied. The proposed simulation results are in good agreement with the theoretical and experimentally measured results proposed in [3, 4].

2. Mathematical Model

The cross-section of a PCF is shown in Figure 1. The PCF is modeled as four circular regions; an air/silica core, an air-silica honeycomb inner cladding consists of array of cylindrical air holes, a solid silica outer cladding, and an acrylate coating. The parameters of each region of the PCF are denoted by a superscript (i = 1, 2, 3, and 4). The acoustic pressure is governed by the wave equation and is given by [13];

$$\frac{1}{\rho_o c^2}\frac{\partial^2 p}{\partial t^2}+\nabla.\left(-\frac{1}{\rho_o}(\nabla p-q)\right)=Q \tag{1}$$

Where t is the time, ρ_o is the density of the fluid, q and Q are the acoustic dipole and monopole source, respectively. The wave equation can be solved in the frequency domain to expand the acoustic signal into harmonic components by its Fourier series. A harmonic solution has the form;

$$p(x,y)=p(x)e^{i\omega t} \tag{2}$$

Where ω is the angular frequency, and the actual physical value of the acoustic pressure is the real part of Eq.(2), consequently, the time-dependent wave equation reduces to the Helmholtz equation given by;

$$\nabla.\left(-\frac{1}{\rho_o}(\nabla p-q)\right)-\frac{\omega^2}{\rho_o c^2}p=Q \tag{3}$$

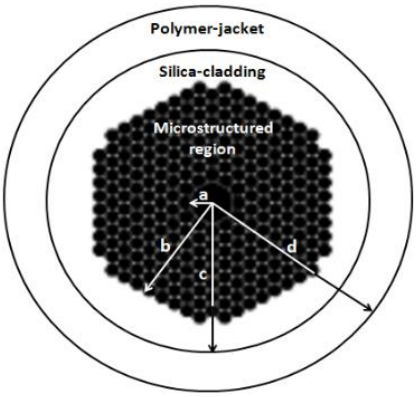

Figure 1. General Cross-Section of a PCF with an Air/Solid Core, Honeycomb Air-Silica Inner Cladding, a Solid Silica Outer Cladding, and a Polymer Coating, where (a-d) Represent the Radius of Each Layer

In the homogenous case where the two source terms q and Q are zero, the solution to the Helmholtz equation is the plane wave given by;

$$p(x,y) = p_o(x)e^{i(\omega t - k.x)} \tag{4}$$

Where p_o is the amplitude of the wave and k is the wave number. Considering each of the investigated fibers as the sensing arm of the interferometric hydrophone, the acoustic pressure (p) primarily affect the fiber length (L), and the effective refractive index of the fundamental mode (n_{eff}) of the phase (φ) of the travelling light through the fiber, where φ is given by;

$$\varphi = \frac{2\pi}{\lambda} n_{eff} L \tag{5}$$

Where λ is the wavelength of the propagating light. To calculate n_{eff}, the FES COMSOL multiphysics is used to solve the vectorial electric field wave equation as an eigenvalue problem and hence to calculate the propagation constant (β), and n_{eff}. NR is a figure of merit independent of wavelength and optical fiber dimensions which is commonly used to compare between different hydrophone designs. It normalizes the sensitivity of the hydrophone ($S=d\varphi/dp$) by the total optical phase shift and for PCFs is given by:

$$NR = \frac{d\varphi}{\varphi(dp)} = \frac{1}{L}\frac{dL}{dp} + \frac{1}{n_{eff}}\frac{dn_{eff}}{dp} = \frac{\varepsilon_z^2}{dp} + \frac{1}{n_{eff}}\frac{dn_{eff}}{dp} \tag{6}$$

where $\varepsilon_z^2 = dL / L$ is the axial strain of the microstructured region of the HC-PBF.

The elasto-optic effect determines the index variation due to applied acoustic pressure. The general linear stress-optical relation is used to calculate the change of n_{eff} due to the applied acoustic pressure and is given by [13, 14]:

$$\begin{aligned} n_x &= n_o - B_1 S_x - B_2(S_y + S_z) \\ n_y &= n_o - B_1 S_y - B_2(S_x + S_z) \\ n_z &= n_o - B_1 S_z - B_2(S_x + S_y) \end{aligned} \tag{7}$$

Where n_o is the refractive index of a stress-free material, B_1 and B_2 are the stress-optic coefficients and S_x, S_y, and S_z are the principal components of the induced stresses in the three directions.

For the conventional SMF, the NR is calculated from [1];

$$\frac{d\varphi}{\varphi dP} = \frac{1}{dP}\left[\varepsilon_z - \frac{n^2}{2}[(p_{11}+p_{12})\varepsilon_r + p_{12}\varepsilon_z]\right] \tag{8}$$

Where ε_z and ε_r are the axial and radial components of strain.

3. Simulation Results and Analysis

In this section, simulation results based on the FES are introduced. The material's physical parameters of the investigated optical fibers shown in Table 1 are imported into the FES. In Table 1, subscripts (1, 2, 3, and 4) represent each region of the optical fiber, d , E, and v are the diameter of the region, the Young's modulus, and the Poisson's ratio of each region, respectively, E_o is the Young's modulus of the silica material. The parameters of the microstructured area of the PCF are: Λ is the pitch (the central distance between two adjacent air-holes in the microstructured cladding), d_h is the diameter of the air-hole, and η is the air-filling ratio (the ratio of d_h to Λ).

Table 1 Physical Parameters of the Investigated Fibers [3, 5, 7, 8]

Region	SMF	LMA-5	HC-1550
Core	Material: $99\%SiO_2+1\%GeO_2$ d_1=8 μm, E_1= 72 GPa, v_1=0.17	Material: Silica d_1 =5 μm, E_o =72 GPa, v_1=0.17	Material: Air d_1= 10.1 μm
Clad	$95\%SiO_2+5\%B_2O_3$ d_2 =125 μm E_2 =72 GPa v_2=0.17	**Air-silica Honeycomb**	**Air-silica Honeycomb**
		d_2 = 38μm, v_2=0.17, Λ=2.9 μm d_h=1.27 μm, η =44% $E_r=E_\theta=(3/2)(1-\eta)^3E_o$ $E_z=(1-\eta)E_o$	d_2 =70 μm, v_2=0.17, Λ=3.8 μm d_h =3.5 μm, η =92% $E_r=E_\theta=(3/2)(1-\eta)^3E_o$ $E_z=(1-\eta)E_o$
		Solid-silica clad	**Solid-silica clad**
		d_3 =125 μm, E_3 =72 GPa, v_3=0.17	d_3 =120 μm, E_3 =72 GPa, v_3=0.17
Polymer coating	Material: Acrylate Thickness (t)=93.5 μm E_3 =0.75 GPa, v_3=0.45	Material: Acrylate t=93.5 μm, E_4 =0.75 GPa, v_4=0.45	Material: Acrylate t =93.5 μm, E_4 =0.75 GPa, v_4=0.45
NR (dB)	-366	-367.5	-344

The response of the HC-PBF to acoustic pressure is studied by coupling between the Acoustic solid-interaction (ASI), and the Wave optics (WOM) modules in the FES. This allows easy transfer of the required data between the two modules, and provides accurate calculations. After setting up the model geometry, and importing the required equations and parameters to the FES, the ASI is used to apply acoustic pressure of different amplitudes and frequencies that cause structural deformation; hence the induced stresses and strains of the investigated fibers are calculated. The ASI exchanges data with the WOM by coupling between them, then by performing mode analysis, n_{eff} corresponding to the deformed structure is calculated. This allows calculating the phase change and NR for the investigated fibers given by Eqs. (5, 6, 8), respectively. The microstructured regions of the PCFs are modeled as anisotropic materials while the silica outer cladding and the acrylate regions are modeled as isotropic materials [11]. The effect of the coating material and thickness on NR was proposed by many researchers and recently in [12]. To avoid inaccurate comparison between the three investigated fibers because of different coating materials and thickness, the same coating material and thickness for all fibers are used. Some data are imported and plotted in MATLAB.

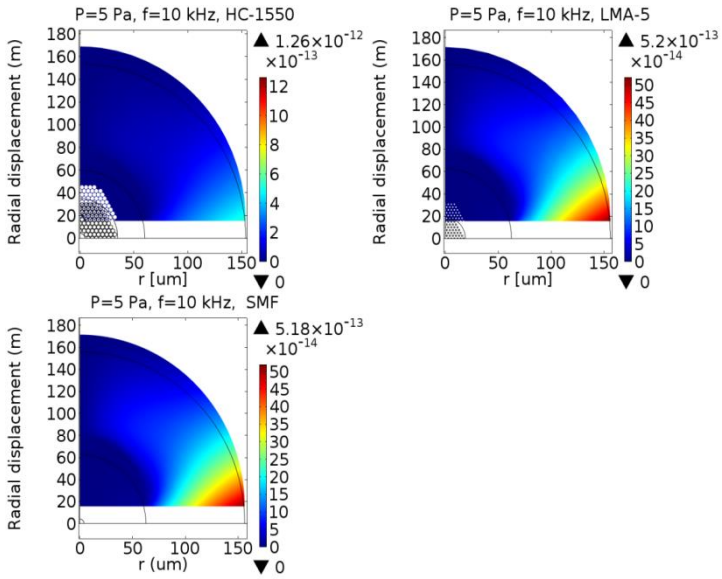

(a) (b) (c)

Figure 2. Radial Displacement Profile for (a) HC-1550, (b) LMA-5, and (c) SMF, for p = 5 Pa, f = 10 kHz.

Figure 2 and Figure 3 show the calculated radial displacement as a function of the optical fiber radius (*r*) for HC-1550, LMA-5, and SMF, for applied acoustic pressure of 5 Pa and acoustic frequency (*f*) of 10 kHz. In Figure 3, the radial displacement data of the HC-1550 is fitted by shape-preserving interpolant in MATLAB.

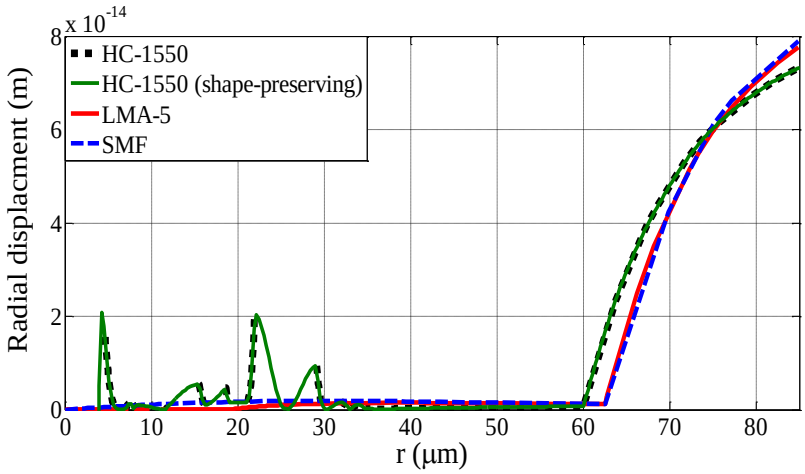

Figure 3. Radial Displacement as a Function of Fiber Radius for (a) HC-1550, (b) LMA-5, and (c) SMF, for p = 5 Pa, f = 10 kHz

It can be seen from Figure 3, that the honeycomb region of the HC-1550 (5< *r* <35 μm) has peaks of displacement values in regions corresponding to the deformed silica between the air holes while the solid-silica region (35< *r* <60 μm) has very small values. The reason for this is the high Young's modulus of the solid-silica material that limits its deformation. From Figure 3, it is shown that despite the presence of the air-holes in the microstructure region of the LMA-5, its radial displacement is approximately the same as that of the SMF. This can be attributed to the presence of the solid-core and the low air-filling ratio of the honeycomb area that limit its ability to deform. For SMF, it can be seen that the displacement in the silica region (0 <*r* <62.5 μm) is generally very small. This can

be attributed to the high Young's modulus of silica material of the core and cladding that limits the flexibility of the material and consequently, the NR of the SMF. Generally, for the three optical fibers the region with the highest radial displacement is the polymer coating region (r >60 μm) in which the acrylate material has low Young's modulus allows it to deform easily. As a conclusion, for the same applied acoustic pressure and frequency the radial displacement of the HC-1550 is higher than the LMA-5 and SMF. This indicates that generally, HC-PBF are more compressive and consequently, have higher sensitivity to acoustic pressure than that of SC-PCF and SMF [3, 15].

We also investigate the effect of changing the structure of the honeycomb region on the axial strain and NR of the HC-1550. Figure 4 shows the axial strain of the HC-1550 versus η for different applied acoustic pressures. In this figure Λ is swept from 3.8 μm to 6.3 μm and allowed to extend to the solid-silica cladding region, while d_h is kept unchanged. From Figure 4, it can be deduced that generally, as η decreases the axial strain decreases. The reason for this is that as Λ increases, the amount of silica in the honeycomb area increases that limits the axial strain. Also, it is shown that as the acoustic pressure and η increase, large deformation occurs in the honeycomb area causes the axial strain to increase noticeably higher than its values when the acoustic pressure is smaller for the same η.

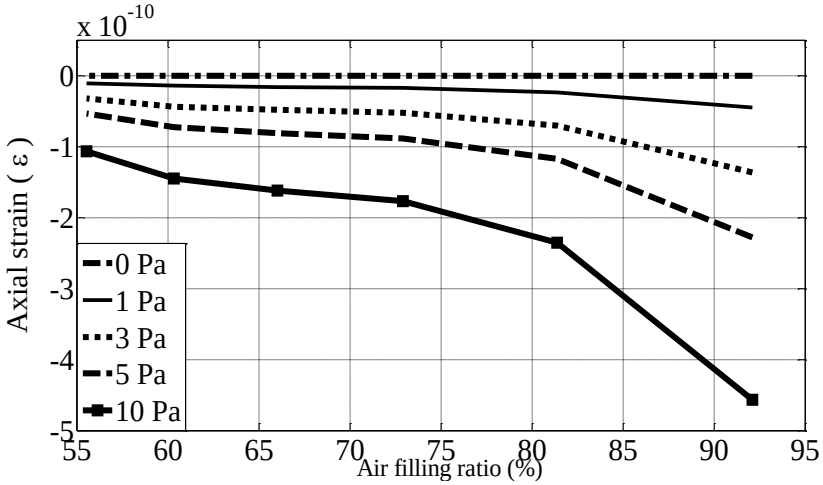

Figure 4. Axial Strain of the Microstructured Region of HC-1550 as a Function of η for Different Acoustic Pressures

The FES enables us to calculate the *NR* of the investigated optical fibers as shown in Figure 5. It can be seen that the calculated average *NR* for applied acoustic pressure of 1 Pa in the frequency range from 10 kHz to 50 kHz for the HC-1550, LMA-5, and SMF are -344 dB,

-367.5 dB, and -366 dB, respectively. HC-1550 has the highest *NR* due to its air-core and the high air-filling ratio in the honeycomb area. This reduces the amount of silica in the honeycomb area, reduces the contribution of the index term of the NR given in Eq. (6) and consequently, increases the *NR*.

In [3], the experimental results showed that the *NR* of HC-1550 is about 15 dB higher than that of the conventional SMF, while the proposed simulation results shows a difference of about 22 dB. We attribute this 7 dB difference to the use of the real structure in [3] that may contains imperfections causes reduction of the *NR* of the HC-1550 compared to the ideal structure that we used in the simulation. Simulation results show that the NR of the LMA-5 is 1.5 dB lower than that of SMF, while it was expected that LMA-5 has better NR because of the presence of the honeycomb cladding that has smaller equivalent Young's modulus than that of the SMF. This can be attributed to the following reasons; (1) the large amount of silica in the honeycomb area because of the

solid-core, and the low air-filling ratio (η = 44%) that limits the ability of LMA-5 to deform, (2) as the light propagates in solid-core, the calculated index term in Eq.(6) is significant and this reduces the overall *NR* of the LMA-5. In addition to the sensitivity to acoustic pressure, size of the sensor is also an important factor. If the SMF and the LMA-5 have about the same NR, then we can take other advantages offered by LMA-5 like bend insensitivity, endlessly single-mode operation, and others [8]. We conclude that even if the LMA-5 and SMF have about the same NR, LMA-5 is preferable as it allows the fabrication of smaller size hydrophones.

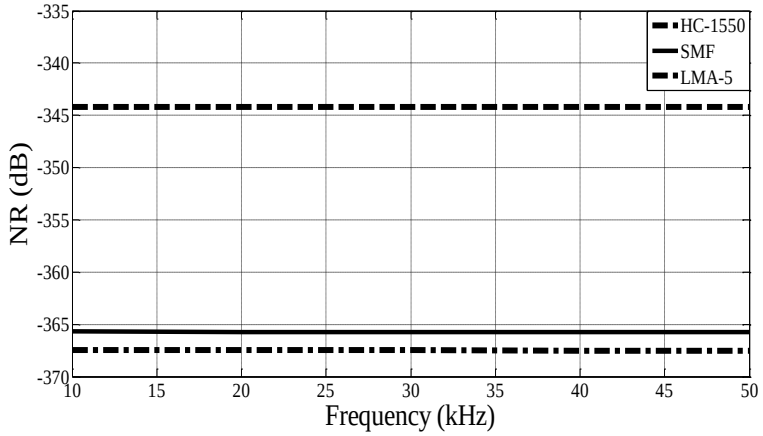

Figure 5. Average NR as a Function of Acoustic Frequency for the HC-1550, LMA-5, and SMF for Acoustic Pressure of 1 Pa

The main structural factors that are responsible for controlling NR of the PCFs are the air-core diameter (d_1), η, the number of hole rings in the honeycomb area, the thickness of the silica outer cladding, and the coating material and thickness. In this study we concentrate on the effect of d_1, and η on NR of HC-1550 in two cases. It was expected that d_1 is the dominant factor that contribute to the high NR of the HC-PBF because it has a large diameter (d_1= 10.1 μm) that reduces the amount of silica in the structure. In both case studies, the diameter of the honeycomb region is kept constant (d_2 =70 μm). The first case study is to keep η unchanged (η = 92%) and calculate NR for the original structure with HC then by replacing the HC with SC. The second case is to change η to 60% and calculate NR with HC then with SC. Figure 6 shows the simulation results of this study where NR of HC-1550 as a function of the acoustic frequency for different aforementioned air-filling ratios is plotted. It can be seen that for the same η, changing the core from HC to SC only reduce the overall NR about 4 dB, while for the same core type but changing η from 92% to 60%, NR is reduced 25 dB. This shows that the dominant structural factor that has greater impact on NR of the PCFs is η than the type of the core.

Based on this study, we propose a mathematical relation between sensitivity to acoustic pressure of the HC-PBF per unit pressure as a function of η, where *S* is related to NR by; $NR_{dB}=S_{dB}-20log(\varphi)$,where $S_{dB}=20log(S)$, and $NR_{dB}=20log(NR)$. Data is imported from COMSOL to MATLAB and fitted by cubic polynomial as it showed minimum fitting error with minimum equation terms. As a result, the following formula is obtained;

$$S = (1.1535\times10^{-9}\eta^3 - 2.061\times10^{-9}\eta^2 + 1.2393\times10^{-9}\eta - 2.4872\times10^{-10}) \quad (9)$$

This formula is useful for the design of HC-PBFs for acoustic pressure sensing.

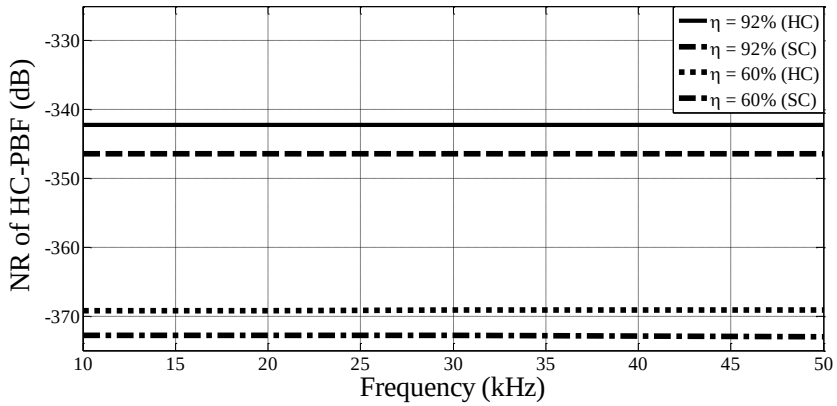

Figure 6. NR of HC-PBF as a Function of the Acoustic Frequency for Different Air-Filling Ratios (HC) Indicates using the Same Structure with Hollow-core, while (SC) Indicates using the Same Structure with Solid-Core

4. Conclusion

As a conclusion, the FES COMSOL multiphysics are used to study and compare the sensitivity to acoustic pressure of HC-1550, LMA-5, and SMF. The proposed simulation results shows that for the same applied acoustic pressure and frequency the sensitivity to acoustic pressure of the HC-1550 is higher than that of LMA-5 and SMF by 23.5 dB and 22 dB, respectively. This is because of its air core and the high air-filling ratio in the honeycomb area that allows the induced axial strain to increase and consequently, the NR. Simulation results showed that despite the presence of the air-holes in the microstructure region of the LMA-5, its sensitivity to acoustic pressure is lower than that of SMF by 1.5 dB. However, LMA-5 has other advantages make them preferable as it can be used to fabricate smaller hydrophone size. We studied the effect of changing the air-filling ratio of the HC-PBF on its NR. It was found out that as Λ increases, the amount of silica in the honeycomb area increases that limits the axial strain and consequently, the *NR* decreases. It was also shown that the dominant structural parameter that is responsible for controlling NR of the HC-PBF is the air-filling ratio such that its change has a greater impact on NR than the other factors. Finally, a mathematical formula describes the relation between *S* and η is proposed.

Acknowledgments

This work is supported by National Natural Science Foundation of China (61102004), and Fundamental Research Funds for the Central Universities.

References

[1]. G. A. Cranch, P. J. Nash and C. K. Kirkendall, "Large-scale remotely interrogated arrays of fiber-optic interferometric sensors for underwater acoustic applications," IEEE Sensors Journal, vol. 3, (**2003**), pp. 19-30.
[2]. N. Albor, J. Herr, S. Mastrogiovanni, F. Mulderrig, L. Nucci, A. Price, D. Remner and J. R. DiWranto, "Comparison of Fiber Optic and Conventional Sensors for Naval Applications" Naval Engineers Journal, vol. 108, **(1996)**, pp. 29-42.
[3]. M. Pang and W. Jin, "Detection of acoustic pressure with hollow-core photonic bandgap fiber," Optics Express, vol. 17, (**2009**), pp. 11088-11097.
[4]. Y. Leguillon, P. Besnard, L. Provino, A. Monteville, D. M´echin, D. Tr´egoat, M. Doisy and F.-X. Launay, "Phase sensitivity to axial strain of microstrustured optical silica fibers," In Proceedings of the 21st International Conference on Optical Fiber Sensors, (**2011**) May, Ottawa, Canada.
[5]. "NKT Photonics website", http://www.nktphotonics.com/hollowcorefibers.

[6]. R. P. D. A. Jackson, A. Dandridge and A. B. Tveten, "Elimination of drift in a single-mode optical fiber interferometer using a piezoelectrically stretched coiled fiber," Applied Optics vol. 19, (**1980**), pp. 2926-2929.
[7]. G. A. Cárdenas, F. C. Fávero and J. Villatoro, "High-Visibility Photonic Crystal Fiber Interferometer as Multifunctional Sensor," Journal of Sensors, vol. 13, (**2013**), pp. 2349-2358.
[8]. J. R. F. M. D. Nielsen, N. A. Mortensen and A. Bjarklev, "Bandwidth comparison of photonic crystal fibers and conventional single-mode fibers," Optical Society of America, vol. 12, (**2004**), pp. 430-435.
[9]. H. K. Kim, M. J. F. Digonnet and G. S. Kino, "Air-Core Photonic-Bandgap Fiber-Optic Gyroscope," Journal of Lightwave Technology, vol. 24, (**2006**), pp. 3169-3174.
[10]. W. Jin, H. F. Xuan and H. L. Ho, "Sensing with hollow-core photonic bandgap fibers," Measurement Science and Technology, vol. 21, (**2010**), pp. 1-12.
[11]. M. Pang, H. F. Xuan, J. Ju and W. Jin, "Influence of strain and pressure to the effective refractive index of the fundamental mode of hollow-core photonic bandgap fibers," Optics Express, vol. 18, (**2010),** pp. 14041-14055.
[12]. F. Yang, W. Jin, H. L. Ho, F. Wang, L. Ma and Y. Hu, "Enhancement of acoustic sensitivity of hollow-core photonic bandgap fibers," Optics Express, vol. 21, (**2013**), pp. 15514-15521.
[13]. COMSOL Multiphysics, "Acoustics module user's guide," **(2013)**.
[14]. M. Szpulak, T. Martynkien and W. Urbanczyk, "Effects of hydrostatic pressure on phase and group modal birefringence in microstructured holey fibers," Applied Optics, vol. 43, (**2004**), pp. 4739-4744.
[15]. T. R. H. N. Lagakos, P. Ehrenfeuchter, J. A. Bucaro and A. Dandridge, "Planar Flexible Fiber-optic Acoustic Sensors," Journal of Lightwave Technology, vol. 8, (**1990),** pp. 1298-1303.

